



**An optimally tuned
GENIE ensemble**

R. Marsh et al.

Title Page

Abstract

Introduction

Conclusions

References

Tables

Figures

⏪

⏩

◀

▶

Back

Close

Full Screen / Esc

Printer-friendly Version

Interactive Discussion



This discussion paper is/has been under review for the journal Geoscientific Model Development (GMD). Please refer to the corresponding final paper in GMD if available.

An optimally tuned ensemble of the “eb_go_gs” configuration of GENIE: parameter sensitivity and bifurcations in the Atlantic overturning circulation

R. Marsh¹, A. Sóbester², E. E. Hart², K. I. C. Oliver¹, N. R. Edwards³, and S. J. Cox²

¹National Oceanography Centre Southampton, University of Southampton, Waterfront Campus, European Way, Southampton SO14 3ZH, UK

²Faculty of Engineering and the Environment, University of Southampton, Southampton SO17 1BJ, UK

³Department of Earth and Environmental Sciences, CEPSAR, The Open University, Milton Keynes MK7 6AA, UK

Received: 24 August 2012 – Accepted: 27 December 2012 – Published: 11 February 2013

Correspondence to: R. Marsh (rm12@soton.ac.uk)

Published by Copernicus Publications on behalf of the European Geosciences Union.

Abstract

The key physical parameters of the “eb_go_gs” configuration of GENIE, an Earth system Model of Intermediate Complexity (EMIC), are tuned using a multi-objective genetic algorithm. An ensemble of 90 parameter sets is tuned using two ocean and two atmospheric state variables as targets. These are “Pareto-optimal”, representing a range of trade-offs between the four tuning targets. For the leading five parameter sets, simulations are further evaluated alongside a simulation with untuned “default” parameters, comparing selected variables and diagnostics that describe the state of the atmosphere, ocean and sea ice. One of these parameter sets is selected for further analysis of the objective function (error) landscape in the vicinity of its tuned values. “Cliffs” along some dimensions motivate closer inspection of corresponding variations in the Atlantic meridional overturning circulation (AMOC). This reveals that bifurcations in the AMOC are highly sensitive to parameters that are not commonly associated with MOC stability. Specifically, the state of the AMOC is sensitive to parameters governing the wind-driven circulation and atmospheric heat transport. Five optimal parameter sets are recommended for future use of GENIE in the configuration presented here.

1 Model calibration and parameter space analysis

Earth System models of full complexity are computationally expensive, due to the resolution of physical and biogeochemical processes on short time and space scales. Relatively small ($O(10)$ -member) ensembles of relatively short (centennial) simulations are commonplace. Simulations and predictions with such models are nonetheless sensitive to the parameters for key unresolved processes, such as turbulent mixing of ocean tracers and cloud physics. The uncertainty due to such parameter sensitivity may be considerable, and is the subject of much ongoing research (Slingo et al., 2009). A range of non-linear behaviour in the Earth system (Lenton et al., 2008) may be likewise sensitive to key parameters, but even less is known of such sensitivities in complex

GMDD

6, 925–956, 2013

An optimally tuned GENIE ensemble

R. Marsh et al.

Title Page

Abstract

Introduction

Conclusions

References

Tables

Figures

◀

▶

◀

▶

Back

Close

Full Screen / Esc

Printer-friendly Version

Interactive Discussion



**An optimally tuned
GENIE ensemble**R. Marsh et al.

[Title Page](#)[Abstract](#)[Introduction](#)[Conclusions](#)[References](#)[Tables](#)[Figures](#)[I◀](#)[▶I](#)[◀](#)[▶](#)[Back](#)[Close](#)[Full Screen / Esc](#)[Printer-friendly Version](#)[Interactive Discussion](#)

models. The comparative computational affordability of Earth system models of intermediate complexity (EMICs) facilitates quantifying their uncertainties due to mixing and transport parameter choices in particular. Additionally, through carefully designed experiments and optimization studies across the space of these parameters, the locations of sub-domains of parameter space within which model behaviour may be regarded as plausible (i.e. neither unphysical nor in unacceptable disagreement with observations) may be identified, yielding insights into these sub-domains and into the optimal composition of ensembles that best enable the meeting of observational targets. Consequently, the dependence of emergent non-linear behaviour on key model parameters may become apparent.

One particular family of EMICs is built using the Grid ENabled Integrated Earth system modelling (GENIE) framework. At the core of many GENIE models is the most basic climate model in which atmosphere, ocean and sea ice all play an active role, configured on a 36×36 equal-area-partitioning of the Earth surface with 16 depth layers in the ocean. This climate core has been used extensively, in studies of past, present and future Earth System dynamics (Cao et al., 2009). In the present study, we report the results from an objective tuning of the most recently documented version of the basic climate model (Marsh et al., 2011). As such, this paper is the second in a series that document the development, evaluation and benchmarking of GENIE.

Edwards and Marsh (2005) reported an early parameter sensitivity study of C-GOLDSTEIN, the predecessor to GENIE, which has almost identical ocean and climate dynamics in a simpler (although less flexible) computational implementation. They used a semi-random ensemble of 1000 simulations, with which they addressed both the inverse problem of parameter estimation, and the direct problem of quantifying the uncertainty due to mixing and transport parameters. Subsequent analysis of the model by Edwards et al. (2010) included a statistical process they described as pre-calibration, referring to the infeasibility of a full Bayesian model calibration. The goal of this effort was the identification of uncontroversially implausible values of certain inputs and outputs. They encountered a region of collapsed Atlantic meridional overturning

circulation, presenting itself as a cliff-edge catastrophe in the freshwater forcing dimension of the input space. They also concluded that the exact location of this implausible subspace is a function of several other model parameters.

The identification of plausible sets was also the goal of the study by Holden et al. (2010), with deterministic emulators for five different aspects of the climate state as the key tool. The plausible ensemble was achieved by building, and then using, a statistical filtering process known as Approximate Bayesian Computation. Emulators appeared in a supporting role in the calibration study by Price et al. (2009), where four observational target sets were selected and a multi-objective, emulator-assisted optimizer was used to identify effective ensembles.

Here we use an updated version of GENIE (Marsh et al., 2011) to probe into the structure of the landscapes of four similar targets, related to ocean and atmosphere prognostic variables, in the space of 13 of the GENIE parameters. A goal is to identify a diverse range of parameter sets, each of which provides a different Pareto-optimal fit to observations representing a different balance of processes, thus providing an effective database for testing robustness when inter-model comparisons are not readily available. We discuss a simple evolutionary heuristic for the fast identification of ensembles that simultaneously optimize these targets, also examining the plausibility of these Pareto-optimal parameter sets through a set of further diagnostics for sea ice and the ocean circulation. One of the five lowest error parameter sets is used to further investigate AMOC sensitivity to selected parameters, with a focus on narrow regions of parameter space that host AMOC bifurcations. Following a brief description of the the model, we outline objective targets and the tuning method. The results of model tuning and analysis of parameter sensitivity are presented sequentially in three parts. We conclude with a discussion of novelties in the method and results presented here.

GMDD

6, 925–956, 2013

An optimally tuned GENIE ensemble

R. Marsh et al.

Title Page

Abstract

Introduction

Conclusions

References

Tables

Figures

⏪

⏩

◀

▶

Back

Close

Full Screen / Esc

Printer-friendly Version

Interactive Discussion



2 The model

The EMIC at the centre of this study is “*eb_go_gs*” configuration of *GENIE-1*, comprising an energy and moisture balance model (EMBM) for the atmosphere, coupled with the Global Ocean Linear Drag Salt and Temperature Equation Integrator (GOLD-STEIN) 3-D ocean model and a dynamic and thermodynamic sea ice model. This setup largely follows that of Edwards and Marsh (2005), but uses an updated model version as integrated into the GENIE framework as described by Marsh et al. (2011). This version, based on GENIE version 2.7.4, includes revised wind forcing. Here, we tune the setup referred to as “3636s16l” by Marsh et al. (2011), a standard model resolution with horizontal resolution of equal-area grid cells of 10 degrees longitudinal extent and 16 depth levels in the ocean, which has been used for a wide range of studies. In the following sub-sections, the three components of “*eb_go_gs*” are outlined briefly.

2.1 Atmosphere

The EMBM represents the atmosphere as a single 2-D layer with an advective-diffusive transport scheme for heat and moisture. The prognostic variables are air temperature and specific humidity, representative of the total atmospheric air column. Planetary albedo and the annual-average wind fields for advective transports are prescribed, while transport and ancillary parameters are typically calibrated using data assimilation techniques. Physical processes represented by the model are greatly simplified, examples are the instantaneous return of continental precipitation to coastal ocean points via a runoff map or the parameterisation of outgoing long wave radiation by an empirical polynomial function. An implicit numerical scheme is used to allow long EMBM timesteps.

2.2 Ocean

GOLDSTEIN comprises a reduced physics (frictional-geostrophic) 3-D ocean model (Edwards et al., 1998) featuring spatially variable drag, realistic global bathymetry, mul-

Title Page

Abstract

Introduction

Conclusions

References

Tables

Figures

◀

▶

◀

▶

Back

Close

Full Screen / Esc

Printer-friendly Version

Interactive Discussion



5 tiple islands, and wind-stress forcing from a prescribed 2-D annual-mean wind-stress forcing field (Edwards and Marsh, 2005; Marsh et al., 2011). The prognostic variables are temperature and salinity. The tracer transport scheme employs an isoneutral and eddy-induced mixing scheme and an efficient convection scheme. Unlike primitive-
equation ocean models, momentum advection and acceleration terms are neglected
in the equation of motion, allowing the use of timesteps which are long relative to those generally used in 3-D ocean models.

2.3 Sea ice

10 The third component of “*eb_go_gs*” is a dynamic and thermodynamic sea-ice model (Edwards and Marsh, 2005; Marsh et al., 2011) (herein referred to as GS). Sea ice is transported with the surface ocean current and is subject to a diffusive process with a strength controlled by a tunable parameter. An implicit numerical scheme for sea-ice transport is available (Marsh et al., 2011) and is used in this study.

3 Objective targets and tuning method

15 Table 1 lists the 13 dimensions of the EMBM – GOLDSTEIN – GS parameter space with respect to which we are investigating the model sensitivities. Twelve of these parameters comprise the set used by Edwards and Marsh (2005). We have added a further atmospheric parameter, r_K , controlling the reduction of meridional heat diffusion over Antarctica and the Southern Ocean south of 56° S, introduced to parameterise the partial isolation of the atmosphere in this region, reducing atmospheric temperatures in the Southern Hemisphere high latitudes (see Appendix A in the publication by Cao et al.,
20 2009 and also Marsh et al., 2011). Further tunable parameters of the “*eb_go_gs*” model have been fixed at their default values for the present study.

25 Table 2 lists the four observational fields that we use to define the targets of the ensemble selection study. These datasets, denoted by $S_{T_{ocn}}$, $S_{S_{ocn}}$, $S_{T_{atm}}$ and $S_{Q_{dry}}$ in what follows, are the same as those used for model-data comparison in Marsh et al. (2011),

An optimally tuned GENIE ensemble

R. Marsh et al.

Title Page

Abstract

Introduction

Conclusions

References

Tables

Figures

◀

▶

◀

▶

Back

Close

Full Screen / Esc

Printer-friendly Version

Interactive Discussion



and are similar to those used in earlier studies. A notable exception to some earlier studies (e.g. Edwards and Marsh, 2005; Price et al., 2009) includes the replacement of the specific atmospheric humidity with a climatology of relative humidity (for reasons discussed in Lenton et al., 2006 and Marsh et al., 2011). The observational data are aligned with the model grid points through linear interpolation. In the case of the 3-D temperature and salinity fields, some of the values for some grid points of the model ocean are filled with the value of the closest available points from the observational fields.

The root-mean-squared (RMS) errors defined by these fields and corresponding output fields from “*eb_go_gs*” for the last year of a 5000-yr spin-up model integration ($s_{T_{\text{ocn}}}$, $s_{S_{\text{ocn}}}$, $s_{T_{\text{atm}}}$ and $s_{Q_{\text{dry}}}$) define four *objective functions*:

$$f_{T_{\text{ocn}}}(\mathbf{x}) = \sqrt{\frac{1}{N_{T_{\text{ocn}}}} \sum_{i=1}^{N_{T_{\text{ocn}}}} \frac{[s_{T_{\text{ocn}}}(\mathbf{x}) - S_{T_{\text{ocn}}}]^2}{\hat{\sigma}_{S_{\text{ocn}}}^2}}, \quad (1)$$

$$f_{S_{\text{ocn}}}(\mathbf{x}) = \sqrt{\frac{1}{N_{S_{\text{ocn}}}} \sum_{i=1}^{N_{S_{\text{ocn}}}} \frac{[s_{S_{\text{ocn}}}(\mathbf{x}) - S_{S_{\text{ocn}}}]^2}{\hat{\sigma}_{S_{\text{ocn}}}^2}}, \quad (2)$$

$$f_{T_{\text{atm}}}(\mathbf{x}) = \sqrt{\frac{1}{N_{T_{\text{atm}}}} \sum_{i=1}^{N_{T_{\text{atm}}}} \frac{[s_{T_{\text{atm}}}(\mathbf{x}) - S_{T_{\text{atm}}}]^2}{\hat{\sigma}_{T_{\text{atm}}}^2}}, \quad (3)$$

**An optimally tuned
GENIE ensemble**

R. Marsh et al.

Title Page	
Abstract	Introduction
Conclusions	References
Tables	Figures
◀	▶
◀	▶
Back	Close
Full Screen / Esc	
Printer-friendly Version	
Interactive Discussion	



and

$$f_{Q_{\text{dry}}}(\mathbf{x}) = \sqrt{\frac{1}{N_{Q_{\text{dry}}} \sum_{i=1}^{N_{Q_{\text{dry}}}} \frac{[S_{Q_{\text{dry}}}(\mathbf{x}) - S_{Q_{\text{dry}}}]^2}{\hat{\sigma}_{Q_{\text{dry}}}^2}}, \quad (4)$$

where $\mathbf{x} = \{W, \kappa_h, \kappa_v, \lambda, \kappa_t, \kappa_q, \beta_T, \beta_q, F_a, l_d, l_s, \kappa_{hi}, r_\kappa\}$, and the 13 dimensions of this vector correspond to the parameters defined in Table 1.

The variance $\hat{\sigma}^2$ in the four expressions above is designed to weight the root mean squared error in a way that makes the values of the four functions approximately comparable. This is the same formulation as used in Price et al. (2009), so the results reported there are directly comparable with ours, except for $f_{Q_{\text{dry}}}$, as indicated earlier. With these functions we formulate a multi-objective search, the goal of which is to build ensembles comprising *non-dominated* parameter sets. Such vectors, also known as *Pareto-optimal* points of the parameter space, have the property that each outperforms all other points in the set along one of the four dimensions of the output space.

This methodology builds on earlier tuning work by Edwards and Marsh (2005), who sampled the entire parameter space of the (pre-GENIE) C-GOLDSTEIN model through a semi-random, space-filling sampling plan of 1000 individual simulations, and used the responses of the model as the basis for parameter sensitivity analysis. The drawback of this approach is poor scalability with increased problem dimensionality: the number of runs required for a factorial design increases exponentially with the number of parameters to be tuned, although even simple Latin hypercube designs (such as used by Edwards and Marsh, 2005) are much more efficient.

Multi-objective evolutionary search methods, such as the one adopted here (similar to that used by Price et al., 2009) are more robust to this *curse of dimensionality* and they are also more readily scalable in terms of the number of targets/constraints. The multi-objective genetic algorithm achieves this by progressively “learning” the plau-

GMDD

6, 925–956, 2013

An optimally tuned GENIE ensemble

R. Marsh et al.

Title Page

Abstract

Introduction

Conclusions

References

Tables

Figures

◀

▶

◀

▶

Back

Close

Full Screen / Esc

Printer-friendly Version

Interactive Discussion



An optimally tuned GENIE ensemble

R. Marsh et al.

Title Page

Abstract

Introduction

Conclusions

References

Tables

Figures

◀

▶

◀

▶

Back

Close

Full Screen / Esc

Printer-friendly Version

Interactive Discussion



sible regions of the search space through a sequence of generations, during which the selective pressure of the optimizer biases each population towards non-dominated individuals. This will, ultimately, result in a fuller understanding of the tuning landscape than a process that either samples uniformly (Edwards and Marsh, 2005) or considers each target (objective function) in isolation, the latter being prone to the risk of biasing the tuning process towards solutions that excel on individual targets, if model structural error is not properly accounted for. Of course, the genetic multi-objective search comes with no mathematical guarantees of convergence (not even to locally non-dominated parameter sets), but experience shows that this class of heuristics is better suited to problems with high dimensionality, especially those that exhibit discontinuities (which, as we shall see, are a feature of the tuning landscape being considered here).

4 Results

We first address the initial generation of non-dominated ensembles of equilibrium solutions and the identification of Pareto fronts in 2-D target space. We then outline the isolation of five equally plausible parameter sets, based on the appraisal of atmospheric and ocean state variables, and three sensitive model diagnostics (2-D fields). Finally, we focus on the sensitivity of the four objective functions and one of these diagnostics to key parameters in the vicinity of one tuned parameter set, exploring features of the “landscape” associated with variations in these parameters.

4.1 Identifying non-dominated ensembles

On a complex, multi-dimensional search space containing islands of implausibility, a standard choice for a multi-objective search heuristic is some type of evolutionary algorithm. These require few assumptions in relation to the shapes of the objective landscapes and their derivatives and promise robust performance even in conditions such as those encountered by Edwards et al. (2010), whose study identified potential dis-

continuities caused by AMOC collapse. The particular heuristic adopted here is the Non-dominated Sorting Genetic Algorithm (NSGA-II, Deb et al., 2002).

Given a CPU time of 2 h and 10 min for a model run with a 5000-yr spin-up and the availability of approximately 90 processors at any one time on the University of Southampton Iridis 3 supercomputer, we opted for a population size of 90 individuals, giving a generation wall-clock time of 2 h 10 min. We ran the ensemble selection search over 20 generations – this yielded the Pareto fronts (or, more specifically, 2-D projections of Pareto fronts) depicted in Fig. 1, which illustrates the relationships between objective functions that measure goodness of fit, or model error.

A noteworthy feature of these fronts is that T_{ocn} and S_{ocn} , as well as T_{ocn} and T_{atm} , appear to be reasonably well correlated in the region of the best objective values, while the shape of the fronts related to the other possible pairings indicates some level of competition between these objective functions. The former correlations can be interpreted physically: correlation of the T_{ocn} and S_{ocn} objective functions is consistent with obtaining water mass properties, temperature and salinity, that are closest to observations; correlation of the T_{ocn} and T_{atm} objective functions is consistent with obtaining a more realistic climate state, as ocean and air temperatures are tightly coupled. The apparent competition between S_{ocn} and Q_{dry} in particular may reflect a trade-off between realism over land or oceans, or between climate zones, so more realistic ocean salinity may be obtained with less realistic land humidity, or more realistic low-latitude salinity may be obtained with less realistic high latitude humidity (and vice versa in both cases). Mapping the Pareto front back into the 13-dimensional parameter space yielded the histograms shown on Fig. 2. Clearly some distributions are bimodal, further suggesting trade-offs between different processes/regions and objective functions.

4.2 An ensemble of five parameter sets

From the 90 Pareto-optimal parameter sets obtained through the multi-objective search we selected five for further analysis, on the basis of their objective function values. Specifically, we have selected points 18, 37, 49, 56, 74, as they were the only sets to

An optimally tuned GENIE ensemble

R. Marsh et al.

Title Page

Abstract

Introduction

Conclusions

References

Tables

Figures

◀

▶

◀

▶

Back

Close

Full Screen / Esc

Printer-friendly Version

Interactive Discussion



An optimally tuned GENIE ensemble

R. Marsh et al.

Title Page

Abstract

Introduction

Conclusions

References

Tables

Figures

◀

▶

◀

▶

Back

Close

Full Screen / Esc

Printer-friendly Version

Interactive Discussion



feature in the top third of the overall objective function ranges of the 90 points against all four of their objectives. The values of the input variables for these 5 points are shown in Table 3. For closer examination of these points, and for comparison with the corresponding Marsh et al. (2011) configuration (using untuned parameters, henceforth GMD11), we evaluate selected variables and diagnostics that describe the state of the atmosphere, ocean and sea ice. Figures S1–12 (Supplement) show simulated, observed and difference (simulated minus observed) fields, for annual-mean surface air temperature and specific humidity (Figs. S1–6), and for annual-mean sea surface temperature and salinity (Figs. S7–12). We show corresponding Taylor diagrams for air temperature (Fig. 3a), specific humidity (Fig. 3b), sea surface temperature (Fig. 3c), sea surface salinity (Fig. 3d), and also for full-depth ocean temperature (Fig. 3e) and salinity (Fig. 3f). Figure 4a through 4e show annual-mean sea ice concentrations and thicknesses for this small ensemble, with Figs. 5a through 5e and 6a through 6e showing respectively the barotropic streamfunction and the Atlantic Meridional Overturning streamfunction. As a reference, Figs. 4f, 5f and 6f show the sea ice variables and ocean circulation streamfunctions for GMD11.

We first consider the atmosphere (Figs. S1–6). The model is cooler than observations at most locations, with particularly large errors in the Eurasian Arctic. Tropical humidities are generally too high, with the particular exception of anomalously low humidities over the eastern subtropical basins for points 18, 49 and 56. The surface ocean is generally characterised by a cold Atlantic sector and a warm/cold dipole in the west/east Pacific, and largest salinity errors at western boundaries and at high latitudes (Figs. S7–12). Differences between the fits of each simulated property distribution to observations are captured in the Taylor diagrams (Fig. 3), where standard deviations of 1.0 correspond to the correct amplitude of property distribution. Parameter tuning both improves and degrades property distributions. Although differences relative to GMD11 are generally small, some are notable. The standard deviation of air temperature is somewhat improved, without compromising correlation, for points 37 and 74. In the case of specific humidity, standard deviation and correlation are degraded at all points,

least so for points 37 and 74. For sea surface temperature, only marginal differences arise in standard deviation and correlation for points 37 and 74. For sea surface salinity, standard deviation is substantially improved, with reduced correlation, for points 18 and 56. As for surface temperature, the fits of full-depth temperature distributions are little altered by tuning. For full-depth salinity, standard deviation is improved for point 18, but standard deviation and correlation are both degraded for points 37, 49 and 74.

Beyond property distributions, we also evaluate aspects of the climate system that are of regional importance and likely to play key roles in the transient response to radiative forcing. We first consider sea ice distributions in the context of observations (National Snow and Ice Data Center, 2010). Points 18 and 74 show reasonable values in the north, but too little sea ice in the south (Fig. 4a, e). Point 37 corresponds to plausible amounts of sea ice in both the north and the south, although both are slightly excessive (Fig. 4b). There is too much sea ice in the north for point 49 yet almost none in the south (Fig. 4c), while northern sea ice is the most excessive for point 56 (Fig. 4d). In contrast to the ensemble of tuned points, sea ice in the southern hemisphere of GMD11 is somewhat excessive (Fig. 4f). The horizontal (barotropic) circulation in GENIE is generally weaker than observations, which indicate a circumpolar transport of 140 ± 6 Sv (Ganachaud and Wunsch, 2000). The Antarctic circumpolar flow is strongest, and hence most realistic, on point 74 (Fig. 5e), although differences between the five points are marginal. In contrast to the ensemble of tuned points, the barotropic circulation of GMD11 is unrealistically weak (Fig. 5f). The Atlantic overturning circulation comprises two meridional cells: an upper cell transporting 15 Sv and an abyssal cell transporting 2 Sv (Ganachaud and Wunsch, 2000). Points 18 and 56 yield the most realistic overturning streamfunctions (Fig. 6a, d). Points 37 and 49 are characterised by overturning streamfunctions that are rather too intense and the southward flow for point 37 extends considerably deeper than is observed (Fig. 6b, c). The overturning corresponding to point 74 is too weak – it is close to collapse (Fig. 6e). Compared to points 18, 37, 49 and 56, the Atlantic overturning of GMD11 is unrealistically weak and shallow (Fig. 6f). To summarize, as a most acceptable compromise

**An optimally tuned
GENIE ensemble**

R. Marsh et al.

[Title Page](#)[Abstract](#)[Introduction](#)[Conclusions](#)[References](#)[Tables](#)[Figures](#)[◀](#)[▶](#)[◀](#)[▶](#)[Back](#)[Close](#)[Full Screen / Esc](#)[Printer-friendly Version](#)[Interactive Discussion](#)

between realism in property distributions, sea ice, horizontal transport and overturning, we judge point 18 to be marginally most plausible. Consequently, in what follows we shall investigate objective landscapes in more detail in the neighbourhood of this point. The parameter set for point 18, encapsulated in the file 3636s16l_spinup_pt18.xml, is listed in Appendix A.

4.3 Features of the landscape in an optimal ensemble member

In order to gain an understanding of the key features of the four objective landscapes (T_{atm} , Q_{dry} , T_{ocn} , S_{ocn}), we have performed a series of 1-parameter sweeps around point 18. The resolution of these sweeps was 180 points per dimension (parameter) and the resulting 1-D sections are shown in Fig. 7.

The most striking feature of these sections through the landscape is the presence of discontinuities in some of the objective function responses. In particular, the variation of salinity with the wind-scale coefficient, the friction coefficient, the moisture diffusivity, the heat advection coefficient and the fresh water flux factor exhibit steep “cliffs”. Such discontinuities are most likely associated with different states of the Atlantic Meridional Overturning Circulation (AMOC). In order to better understand the causes behind this phenomenon (also observed by Marsh et al., 2004 and Edwards et al., 2010), we therefore investigate AMOC state in the neighbourhoods of these discontinuities.

In particular, we examine two metrics of the AMOC: (i) maximum (positive) intensity of the upper cell, representing the extent of northern sinking (the outflow of dense water formed in the North Atlantic), (ii) minimum (negative) intensity of the lower cell, representing the extent of southern sinking (the inflow of dense water formed around Antarctica). These metrics are investigated either side of each cliff, as a function of the wind scale coefficient, the friction coefficient, the moisture diffusivity, the heat advection coefficient and the fresh water flux. These “one-factor-at-a-time” studies, performed at a resolution of 180 points, cover the immediate neighbourhood of the cliffs. Figure 8 shows “noise” in the transition across the cliff. The existence of such AMOC-transport cliffs in parameter space, associated with large scale ocean fresh water transport, has

An optimally tuned GENIE ensemble

R. Marsh et al.

Title Page

Abstract

Introduction

Conclusions

References

Tables

Figures

◀

▶

◀

▶

Back

Close

Full Screen / Esc

Printer-friendly Version

Interactive Discussion



An optimally tuned GENIE ensemble

R. Marsh et al.

Title Page

Abstract

Introduction

Conclusions

References

Tables

Figures

◀

▶

◀

▶

Back

Close

Full Screen / Esc

Printer-friendly Version

Interactive Discussion



long been recognised both in GENIE (Edwards and Marsh, 2005; Marsh et al., 2004; Lenton et al., 2006), and in other models. To our knowledge, the characterisation of this transition by fine resolution sampling of parameter space is novel. We find that the so-called cliff is instead a series of peaks (representing AMOC-on states) and troughs (representing AMOC-off states) separating the flatter regions either side of the transition. Within the transition region, there is a strong non-monotonic dependence of steady state AMOC on parameters expected to control the AMOC (moisture diffusivity and the freshwater flux factor), as well as parameters that are not traditionally associated with AMOC stability (wind scale coefficient, friction coefficient and atmospheric heat advection coefficient). Therefore, in this region, even the sign of the gradient $\partial\psi/\partial p_n$, where ψ is the steady state AMOC transport and p_n is the value of parameter n , is not predictable from a general understanding of controls on the AMOC.

In interpreting these results, we emphasise that these were obtained despite the use of identical initial conditions for all simulations, and despite the absence of a dynamical atmosphere or of mesoscale ocean processes recognised to give rise to chaos in climate models. It has previously been shown that $\partial\psi/\partial p_n$ undergoes frequent changes of sign within GENIE (Stephenson, 2010), likely associated with localised non-linearities in the model such as the onset or otherwise of convection within a given region of the ocean. However, the associated vacillations in AMOC transport were of sufficiently small amplitude to be negligible if large amplitude changes in p_n were considered. Similar small vacillations can be observed in Fig. 8, but these vacillations attain leading order importance, in some cases exceeding 10 Sv, within the transition region. We postulate that this is due to amplification of the existing vacillations in the presence of a larger scale bifurcation.

5 Conclusions

A multi-objective genetic algorithm has been used to tune the key physical parameters of the climate core for an earth system model of intermediate complexity (GENIE), pre-

An optimally tuned GENIE ensemble

R. Marsh et al.

Title Page

Abstract

Introduction

Conclusions

References

Tables

Figures

◀

▶

◀

▶

Back

Close

Full Screen / Esc

Printer-friendly Version

Interactive Discussion



viously described in Marsh et al. (2011). An ensemble of 90 parameter sets was tuned using two ocean and two atmospheric state variables as targets, defining four objective error functions. Alongside the corresponding Marsh et al. (2011) configuration (using untuned parameters), a sub-ensemble of five Pareto-optimal parameter sets was identified for more subjective evaluation of key variables and diagnostics (surface atmosphere/ocean properties, sea ice distributions and ocean circulation streamfunctions). While statistical analysis of surface property patterns suggest only marginal improvements over the untuned configuration, it was evident that sea ice and ocean circulation – key determinants of the transient climate response under radiative forcing – are more realistic after tuning, at selected points. One of the Paereto-optimal parameter sets was subsequently selected for further analysis of the objective function landscape in the vicinity of its tuned values.

“Cliffs” in the landscape are attributed to variation of the Atlantic Meridional Overturning Circulation (AMOC). The model AMOC is found to be highly sensitive to parameters in proximity to a bifurcation point, manifest as vacillation between “on” and “off” AMOC states. The absence of strong AMOC variability for corresponding parameter values suggests that here the AMOC is in a bistable regime. This finding is complementary to previous studies that specifically addressed AMOC bistability through more extensive but less efficient parameter sweeps (Marsh et al., 2004; Lenton et al., 2006). While such studies have shown that AMOC transitions are abrupt, our fine sampling of parameter space has revealed that they are not monotonic, but are instead characterised by a region within which the dependence of AMOC transport on model parameters is highly unpredictable. Our results suggest that the limited predictability of the large scale oscillation close to bifurcation (Knutti and Stocker, 2002) is a consequence of the location of the bifurcation being poorly defined, rather than simply uncertain or inadequately resolved by the model physics.

In summary, we have presented a tuning and evaluation of the climate core of GENIE, providing a range of plausible tuned parameter sets, and demonstrated that AMOC stability in GENIE is highly sensitive to a surprising range of model parameters.

Appendix A

Phase 1a XML

```
<?xml version="1.0" encoding="UTF-8"?>
<job>
  <vars>
<var name="EXPID">rel-2-7-4-tuning-1a</var>
  </vars>
  <config>
    <model name="goldstein"/>
    <model name="goldsteinseaiice"/>
    <model name="embm"/>
    <model name="wind"/>
  </config>
  <parameters>
    <control>
      <param name="kocn.loop">5</param>
      <param name="ksic.loop">5</param>
      <param name="write.flag.atm">.false.</param>
      <param name="koverall.total">2400000</param>
      <param name="genie.timestep">65745</param>
      <param name="write.flag.sic">.false.</param>
      <param name="dt.write">2400000</param>
      <param name="lgraphics">.false.</param>
    </control>
    <model name="goldstein">
      <param name="ans">n</param>
      <param name="nyear">96</param>
      <param name="npstp">480000</param>
      <param name="iwstp">480000</param>
      <param name="ianav">480000</param>
      <param name="itstp">96</param>
      <param name="netout">n</param>
      <param name="ascout">y</param>
      <param name="lout">spn</param>
      <param name="world">worjh2</param>
      <param name="scf">1.531013488769531300</param>
      <param name="rel">0.9000000</param>
      <param name="temp1">0.0</param>
      <param name="temp0">0.0</param>
      <param name="adrag">2.710164785385131800</param>
      <paramArray name="diff">
<param index="2">0.000025363247914356</param>
<param index="1">1494.438354492187500000</param>
      </paramArray>
      <param name="ieos">1</param>
      <param name="imld">0</param>
      <param name="tdatafile">WOA05.an.TS.nc</param>
      <param name="sdatafile">WOA05.an.TS.nc</param>
      <param name="tsinterp">.true.</param>
      <param name="tdata.varname">t00an1</param>
      <param name="tdata.missing">1.0e20</param>
      <param name="tdata.scaling">1.0</param>
    </model>
  </parameters>
</job>
```

GMDD

6, 925–956, 2013

An optimally tuned GENIE ensemble

R. Marsh et al.

Title Page

Abstract

Introduction

Conclusions

References

Tables

Figures

◀

▶

◀

▶

Back

Close

Full Screen / Esc

Printer-friendly Version

Interactive Discussion



GMDD

6, 925–956, 2013

An optimally tuned
GENIE ensemble

R. Marsh et al.

```

<param name="tdata_offset">0.0</param>
<param name="sdata_varname">s00an1</param>
<param name="sdata_missing">1.0e20</param>
<param name="sdata_scaling">1.0</param>
<param name="sdata_offset">0.0</param>
</model>
<model name="goldsteinseai">
  <param name="ans">n</param>
  <param name="nyear">96</param>
  <param name="npstp">480000</param>
  <param name="iwstp">480000</param>
  <param name="ianav">480000</param>
  <param name="itstp">96</param>
  <param name="ascout">y</param>
  <param name="netout">n</param>
  <param name="lout">spn</param>
  <param name="world">worjh2</param>
  <param name="diffsic">3573.718017578125000000</param>
</model>
<model name="embm">
  <param name="ans">n</param>
  <param name="nyear">96</param>
  <param name="npstp">480000</param>
  <param name="iwstp">480000</param>
  <param name="ianav">480000</param>
  <param name="diffa_len">3</param>
  <param name="netout">n</param>
  <param name="ascout">y</param>
  <param name="lout">spn</param>
  <param name="world">worjh2</param>
  <param name="scl_fwf">0.726862013339996340</param>
  <param name="difflin">0.090003050863742828</param>
  <param name="diffwid">1.410347938537597700</param>
  <param name="scf">1.531013488769531300</param>
  <param name="diffa_scl">0.25</param>
  <param name="itstp">96</param>
  <paramArray name="diffamp">
<param index="2">1173269.250000000000000000</param>
<param index="1">5204945.000000000000000000</param>
  </paramArray>
  <paramArray name="betaz">
<param index="1">0.001037851092405617</param>
<param index="2">0.164652019739151000</param>
  </paramArray>
  <paramArray name="betam">
<param index="1">0.0000000E+00</param>
<param index="2">0.164652019739151000</param>
  </paramArray>
  <param name="tdatafile">NCEP-DOE_Reanalysis_2.ltaa.1000mb.Tr.nc</param>
  <param name="qdatafile">NCEP-DOE_Reanalysis_2.ltaa.1000mb.Tr.nc</param>
  <param name="tqinterp">.true.</param>
  <param name="tdata_varname">air</param>
  <param name="tdata_missing">32766.0</param>
  <param name="tdata_scaling">1.0</param>
  <param name="tdata_offset">273.15</param>
  <param name="qdata_varname">rhum</param>
  <param name="qdata_missing">32766.0</param>

```

Title Page

Abstract

Introduction

Conclusions

References

Tables

Figures

◀

▶

◀

▶

Back

Close

Full Screen / Esc

Printer-friendly Version

Interactive Discussion



An optimally tuned
GENIE ensemble

R. Marsh et al.

Title Page

Abstract

Introduction

Conclusions

References

Tables

Figures

◀

▶

◀

▶

Back

Close

Full Screen / Esc

Printer-friendly Version

Interactive Discussion

```

<param name="qdata_scaling">100.0</param>
<param name="qdata_offset">0.0</param>
<param name="qdata_rhum">.true.</param>
</model>
<model name="wind">
<param name="indir_path"><varref>RUNTIME_ROOT</varref><sep/>genie-wind<sep/>data<sep/>input</param>
<param name="wind_speed_dataset_file">NCEP-DOE_Reanalysis.2.ltaa.1000mb.wind_speed.nc</param>
<param name="wind_speed_dataset_zonal_var">uwnd</param>
<param name="wind_speed_dataset_meridional_var">vwnd</param>
<param name="wind_speed_dataset_missing">32766.0</param>
<param name="wind_speed_dataset_scaling">1.0</param>
<param name="wind_stress_dataset_file">NCEP-DOE_Reanalysis.2.ltaa.wind_stress.nc</param>
<param name="wind_stress_dataset_zonal_var">uflx</param>
<param name="wind_stress_dataset_meridional_var">vflx</param>
<param name="wind_stress_dataset_missing">32766.0</param>
<param name="wind_stress_dataset_scaling">-1.0</param>
</model>
</parameters>
<build>
<make_arg name="IGCMATMOSDP">TRUE</make_arg>
<make_arg name="GENIEDP">TRUE</make_arg>
<macro handle="GENIENXOPTS" status="defined">
<identifier>GENIENX</identifier>
<replacement>36</replacement>
</macro>
<macro handle="GOLDSTEINNLNSOPTS" status="defined">
<identifier>GOLDSTEINNLNS</identifier>
<replacement>36</replacement>
</macro>
<macro handle="GOLDSTEINNLATSOPTS" status="defined">
<identifier>GOLDSTEINNLATS</identifier>
<replacement>36</replacement>
</macro>
<macro handle="GOLDSTEINNLVSOPTS" status="defined">
<identifier>GOLDSTEINNLVLS</identifier>
<replacement>16</replacement>
</macro>
<macro handle="GOLDSTEINNTRACSOPTS" status="defined">
<identifier>GOLDSTEINNTRACS</identifier>
<replacement>2</replacement>
</macro>
<macro handle="GOLDSTEINNISLESOPTS" status="defined">
<identifier>GOLDSTEINNISLES</identifier>
<replacement>1</replacement>
</macro>
<macro handle="GENIENYOPTS" status="defined">
<identifier>GENIENY</identifier>
<replacement>36</replacement>
</macro>
<macro handle="GENIENLOPTS" status="defined">
<identifier>GENIENL</identifier>
<replacement>1</replacement>
</macro>
</build>
<testing>
</testing>
</job>

```



The full set of five selected parameters sets can be accessed online at: <http://www.southampton.ac.uk/~as7/gmd-2012-74/>.

Supplementary material related to this article is available online at:
<http://www.geosci-model-dev-discuss.net/6/925/2013/gmdd-6-925-2013-supplement.pdf>.

Acknowledgements. Genie-LAMP was funded by the Natural Environment Research Council. Robert Marsh acknowledges the support of the Leverhulme Trust during the completion of this manuscript. András Sóbester's work was funded by the Royal Academy of Engineering and the Engineering and Physical Sciences Research Council under their Research Fellowship scheme. The "OptionsRSM" technology and the "Options NSGA-II" toolbox have been supplied by dezineforce and Rolls-Royce (under the VIVACE project) respectively. The simulations were run on the University of Southampton Iridis3 supercomputer. We would also like to thank Ivan I. Voutchkov for helpful suggestions regarding the implementation of the multi-objective search algorithm. Neil Edwards acknowledges financial support from EU FP7 grant no. 265170 (ER-MITAGE). The authors also acknowledge Simon Mueller's help in performing the experiments described in this paper.

References

- Antonov, J. I., Locarnini, R. A., Boyer, T. P., Mishonov, A. V., and Garcia, H. E.: World Ocean Atlas 2005, Volume 2: Salinity. S. Levitus, Ed. NOAA Atlas NESDIS 62, U.S. Government Printing Office, Washington, D.C., 182 pp., 2006. 947
- Cao, L., Eby, M., Ridgwell, A., Caldeira, K., Archer, D., Ishida, A., Joos, F., Matsumoto, K., Mikolajewicz, U., Mouchet, A., Orr, J. C., Plattner, G.-K., Schlitzer, R., Tokos, K., Totterdell, I., Tschumi, T., Yamanaka, Y., and Yool, A.: The role of ocean transport in the uptake of anthropogenic CO₂, *Biogeosciences*, 6, 375–390, doi:10.5194/bg-6-375-2009, 2009. 927, 930

GMDD

6, 925–956, 2013

An optimally tuned GENIE ensemble

R. Marsh et al.

Title Page

Abstract

Introduction

Conclusions

References

Tables

Figures

◀

▶

◀

▶

Back

Close

Full Screen / Esc

Printer-friendly Version

Interactive Discussion



An optimally tuned GENIE ensemble

R. Marsh et al.

Title Page

Abstract

Introduction

Conclusions

References

Tables

Figures

◀

▶

◀

▶

Back

Close

Full Screen / Esc

Printer-friendly Version

Interactive Discussion



- Deb, K., Pratap, A., Agarwal, S., and Meyarivan, T.: A fast and elitist multiobjective genetic algorithm: NSGA-II, *IEEE T. Evolut. Comput.*, 6, 182–197, doi:10.1109/4235.996017, 2002. 934
- Edwards, N. R. and Marsh, R.: Uncertainties due to transport-parameter sensitivity in an efficient 3-D ocean-climate model, *Clim. Dynam.*, 24, 415–433, doi:10.1007/s00382-004-0508-8, 2005. 927, 929, 930, 931, 932, 933, 938
- Edwards, N. R., Willmott, A. J., and Killworth, P. D.: On the role of topography and wind stress on the stability of the thermohaline circulation, *J. Phys. Oceanogr.*, 28, 756–778, 1998. 929
- Edwards, N. R., Cameron, D., and Rougier, J.: Precalibrating an intermediate complexity climate model, *Clim. Dynam.*, 37, 1469–1482, doi:10.1007/s00382-010-0921-0, 2010. 927, 933, 937
- Ganachaud, A. and Wunsch, C.: Improved estimates of global ocean circulation, heat transport and mixing from hydrographic data, *Nature*, 408, 453–457, 2000. 936
- Holden, P., Edwards, N., Oliver, K., Lenton, T., and Wilkinson, R.: A probabilistic calibration of climate sensitivity and terrestrial carbon change in GENIE-1, *Clim. Dynam.*, 35, 785–806, doi:10.1007/s00382-009-0630-8, 2010. 928
- Kanamitsu, M., Ebisuzaki, W., Woollen, J., Yang, S.-K., Hnilo, J. J., Fiorino, M., and Potter, G. L.: NCEP-DOE AMIP-II Reanalysis (R-2). *Bull. Amer. Met. Soc.*, 83, 1631–1643., 2002. 947
- Knutti, R. and Stocker, T. F.: Limited Predictability of the Future Thermohaline Circulation Close to an Instability Threshold, *J. Climate*, 15, 179–186, doi:10.1175/1520-0442(2002)015<0179:LPOFTF>2.0.CO;2, 2002. 939
- Lenton, T. M., Williamson, M., Edwards, N., Marsh, R., Price, A., Ridgwell, A., Shepherd, J., Cox, S., and the GENIE team: Millennial timescale carbon cycle and climate change in an efficient Earth system model, *Clim. Dynam.*, 26, 687–711, doi:10.1007/s00382-006-0109-9, 2006. 931, 938, 939
- Lenton, T. M., Held, H., Kriegler, E., Hall, J. W., Lucht, W., Rahmstorf, S., and Schellnhuber, H. J.: Tipping elements in the Earth’s climate system, *P. Natl. Acad. Sci. USA*, 105, 1786–1793, doi:10.1073/pnas.0705414105, 2008. 926
- Locarnini, R. A., Mishonov, A. V., Antonov, J. I., Boyer, T. P., and Garcia, H. E.: *World Ocean Atlas 2005, Volume 1: Temperature*. S. Levitus, Ed. NOAA Atlas NESDIS 61, U.S. Government Printing Office, Washington, D.C., 182 pp., 2006. 947
- Marsh, R., Yool, A., Lenton, T. M., Gulamali, M. Y., Edwards, N. R., Shepherd, J. G., Krznaric, M., Newhouse, S., and Cox, S. J.: Bistability of the thermohaline circulation identified through

An optimally tuned GENIE ensemble

R. Marsh et al.

Title Page

Abstract

Introduction

Conclusions

References

Tables

Figures

⏪

⏩

◀

▶

Back

Close

Full Screen / Esc

Printer-friendly Version

Interactive Discussion



comprehensive 2-parameter sweeps of an efficient climate model, *Clim. Dynam.*, 23, 761–777, doi:10.1007/s00382-004-0474-1, 2004. 937, 938, 939

Marsh, R., Müller, S. A., Yool, A., and Edwards, N. R.: Incorporation of the C-GOLDSTEIN efficient climate model into the GENIE framework: “eb_go_gs” configurations of GENIE, *Geosci. Model Dev.*, 4, 957–992, doi:10.5194/gmd-4-957-2011, 2011. 927, 928, 929, 930, 931, 935, 939

National Snow and Ice Data Center: Sea Ice Index, Archived Monthly Sea Ice Data and Images, http://nsidc.org/data/seaice_index/archives/index.html (last access: February 2013), 2010. 936

Price, A. R., Myerscough, R. J., Voutchkov, I. I., Marsh, R., and Cox, S. J.: Multi-objective optimization of GENIE Earth system models, *Philos. T. R. Soc. A*, 367, 2623–2633, 2009. 928, 931, 932

Slingo, J., Bates, K., Nikiforakis, N., Piggott, M., Roberts, M., Shaffrey, L., Stevens, I., Vidale, P., and Weller, H.: Developing the next-generation climate system models: challenges and achievements, *Philos. T. R. Soc. A*, 367, 815–831, doi:10.1098/rsta.2008.0207, 2009. 926

Stephenson, G.: Using Derivative Information in the Statistical Analysis of Computer Models, Ph.D. thesis, University of Southampton, 197 pp., 2010. 938

An optimally tuned
GENIE ensemble

R. Marsh et al.

Title Page

Abstract

Introduction

Conclusions

References

Tables

Figures

I◀

▶I

◀

▶

Back

Close

Full Screen / Esc

Printer-friendly Version

Interactive Discussion

**Table 1.** The GENIE parameter space.

Var. no.	Parameter	Notation	Minimum	Maximum	Units
Ocean					
1.	Wind scale coefficient	W	1	3	–
2.	Isopycnal diffusivity	κ_h	1×10^2	1×10^4	$\text{m}^2 \text{s}^{-1}$
3.	Diapycnal diffusivity	κ_v	2×10^{-6}	2×10^{-4}	$\text{m}^2 \text{s}^{-1}$
4.	Inverse friction coefficient	λ^{-1}	0.5	5	days^{-1}
Atmosphere					
5.	Heat diffusivity	κ_t	1×10^6	1×10^7	$\text{m}^2 \text{s}^{-1}$
6.	Moisture diffusivity	κ_q	5×10^4	5×10^6	$\text{m}^2 \text{s}^{-1}$
7.	Heat advection coefficient	β_T	0	1	–
8.	Moisture advection coefficient	β_q	0	1	–
9.	Fresh water flux factor	F_a	0	1	–
10.	Heat diffusivity width	l_d	0.5	2	radians
11.	Heat diffusivity slope	l_s	0	0.25	–
13.	Meridional heat diffusion reduction south of 56° S	r_κ	0	1	–
Sea ice					
12.	Sea ice diffusivity	κ_{hi}	1×10^2	1×10^5	$\text{m}^2 \text{s}^{-1}$

An optimally tuned
GENIE ensemble

R. Marsh et al.

Table 2. Observational target data for the calculation of the objectives. Oceanic properties are from the World Ocean Atlas 2005 (WOA05; http://www.nodc.noaa.gov/OC5/WOA05/pr_woa05.html; Antonov et al., 2006; Locarnini et al., 2006) from the National Oceanographic Data Center (NODC; <http://www.nodc.noaa.gov/>). NCEP_Reanalysis 2 data (Kanamitsu et al., 2002) provided by the NOAA/OAR/ESRL PSD, Boulder, Colorado, USA, from their Web site at <http://www.esrl.noaa.gov/psd/> was used to compute the climatologies of the atmospheric properties.

	Model field	Notation	Units	Climatology	Observational reanalysis data product
Ocean	Temperature	$S_{T_{\text{ocn}}}$	°C	Annual average	World Ocean Atlas 2005 (Antonov et al., 2006)
	Salinity	$S_{S_{\text{ocn}}}$	pss	Annual average	World Ocean Atlas 2005 (Locarnini et al., 2006)
Atmosphere	Temperature	$S_{T_{\text{atm}}}$	°K	Long-term annual average (1979–2010) at 1000 mb level	NCEP_Reanalysis 2 (Kanamitsu et al., 2002)
	Relative humidity	$S_{Q_{\text{dry}}}$	%	Long-term annual average (1979–2010) at 1000 mb level	NCEP_Reanalysis 2 (Kanamitsu et al., 2002)

Title Page

Abstract

Introduction

Conclusions

References

Tables

Figures

◀

▶

◀

▶

Back

Close

Full Screen / Esc

Printer-friendly Version

Interactive Discussion



An optimally tuned
GENIE ensemble

R. Marsh et al.

Table 3. Parameter values for the five “best” points. See Table 1 for parameter definitions and units.

Variable		Point No.					Units
		18	37	49	56	74	
1	W	2.367	2.363	2.367	2.500	2.363	–
2	κ_h	5.54×10^3	5.45×10^3	5.54×10^3	5.45×10^3	5.54×10^3	$\text{m}^2 \text{s}^{-1}$
3	κ_v	4.45×10^{-5}	2.54×10^{-5}	1.43×10^{-4}	5.46×10^{-5}	4.45×10^{-5}	$\text{m}^2 \text{s}^{-1}$
4	λ^{-1}	4.161	4.941	4.161	4.161	4.8.3	days^{-1}
5	κ_t	5.11×10^6	4.09×10^6	3.98×10^6	3.98×10^6	3.98×10^6	$\text{m}^2 \text{s}^{-1}$
6	κ_q	1.95×10^6	1.18×10^6	1.95×10^6	1.95×10^6	1.17×10^6	$\text{m}^2 \text{s}^{-1}$
7	β_T	1.04×10^{-3}	1.04×10^{-3}	1.28×10^{-3}	1.04×10^{-3}	1.04×10^{-3}	–
8	β_q	0.844	0.430	0.842	0.841	0.415	–
9	F_a	0.976	0.886	0.852	0.852	0.635	–
10	l_d	1.143	1.174	1.214	1.120	1.115	radians
11	l_s	0.120	0.057	0.026	0.057	0.120	–
12	κ_{hi}	3.65×10^4	9.88×10^4	9.88×10^4	9.92×10^4	6.99×10^3	$\text{m}^2 \text{s}^{-1}$
13	r_κ	0.764	0.830	0.756	0.861	0.754	–

Title Page

Abstract

Introduction

Conclusions

References

Tables

Figures

◀

▶

◀

▶

Back

Close

Full Screen / Esc

Printer-friendly Version

Interactive Discussion



An optimally tuned GENIE ensemble

R. Marsh et al.

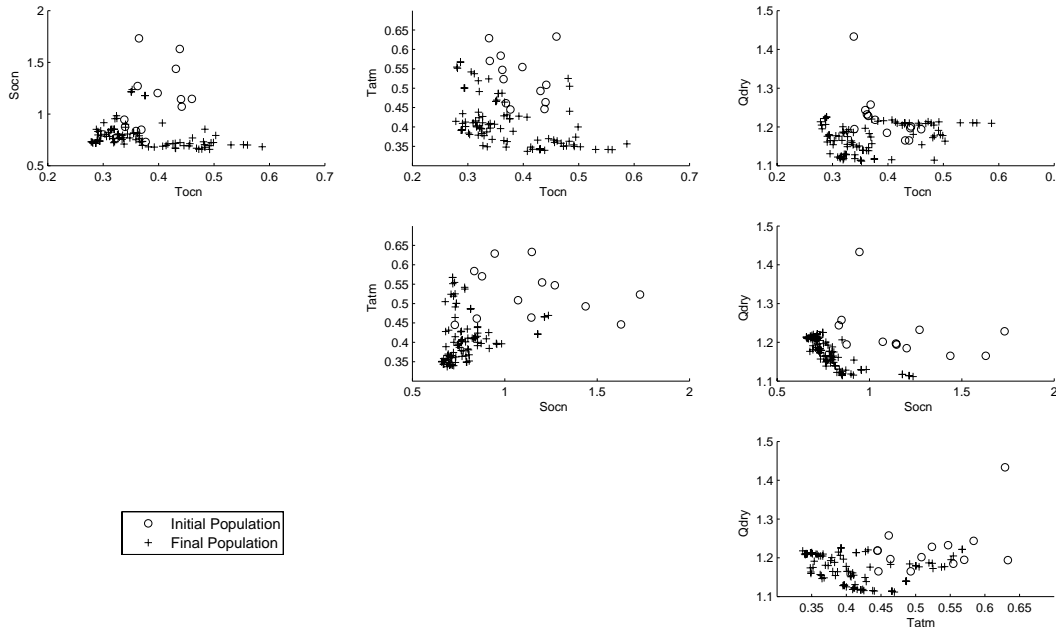


Fig. 1. Scatter plots for each pair of objective function values, for the 90 non-dominated vectors, prior to and following tuning. Note the relatively small number of successful runs in the first generation – hence the considerably fewer than 90 circles on each plot.

[Title Page](#)
[Abstract](#) [Introduction](#)
[Conclusions](#) [References](#)
[Tables](#) [Figures](#)
[◀](#) [▶](#)
[◀](#) [▶](#)
[Back](#) [Close](#)
[Full Screen / Esc](#)
[Printer-friendly Version](#)
[Interactive Discussion](#)



An optimally tuned GENIE ensemble

R. Marsh et al.

Title Page

Abstract

Introduction

Conclusions

References

Tables

Figures



Back

Close

Full Screen / Esc

Printer-friendly Version

Interactive Discussion

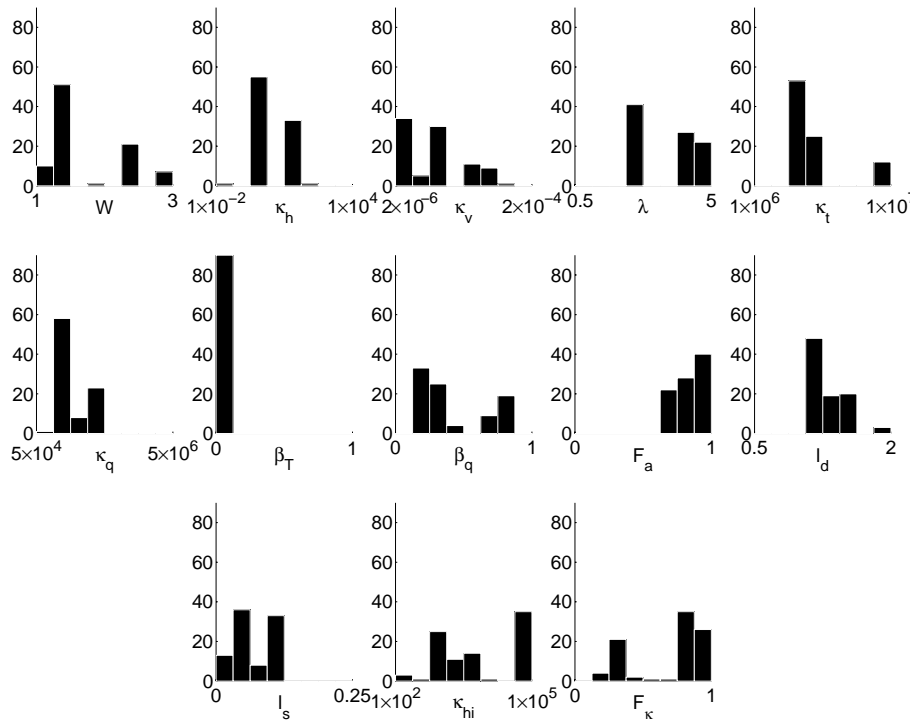


Fig. 2. Ordinary histograms of parameter values across the 90 Pareto-optimal designs. See Table 1 for parameter definitions and units.

An optimally tuned
GENIE ensemble

R. Marsh et al.

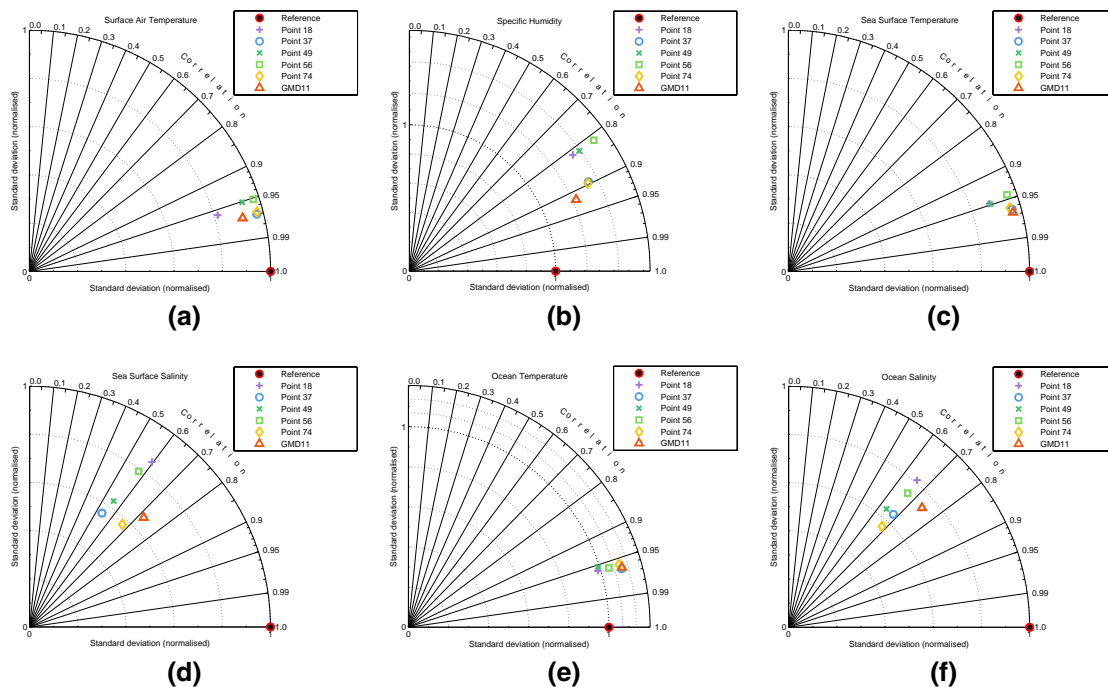


Fig. 3. Taylor diagram of (a) air temperature T_{atm} , (b) specific humidity, (c) sea surface temperature, (d) sea surface salinity, (e) ocean temperature T_{ocn} , and (f) ocean salinity S_{ocn} .

[Title Page](#)
[Abstract](#)
[Introduction](#)
[Conclusions](#)
[References](#)
[Tables](#)
[Figures](#)
[⏪](#)
[⏩](#)
[◀](#)
[▶](#)
[Back](#)
[Close](#)
[Full Screen / Esc](#)
[Printer-friendly Version](#)
[Interactive Discussion](#)

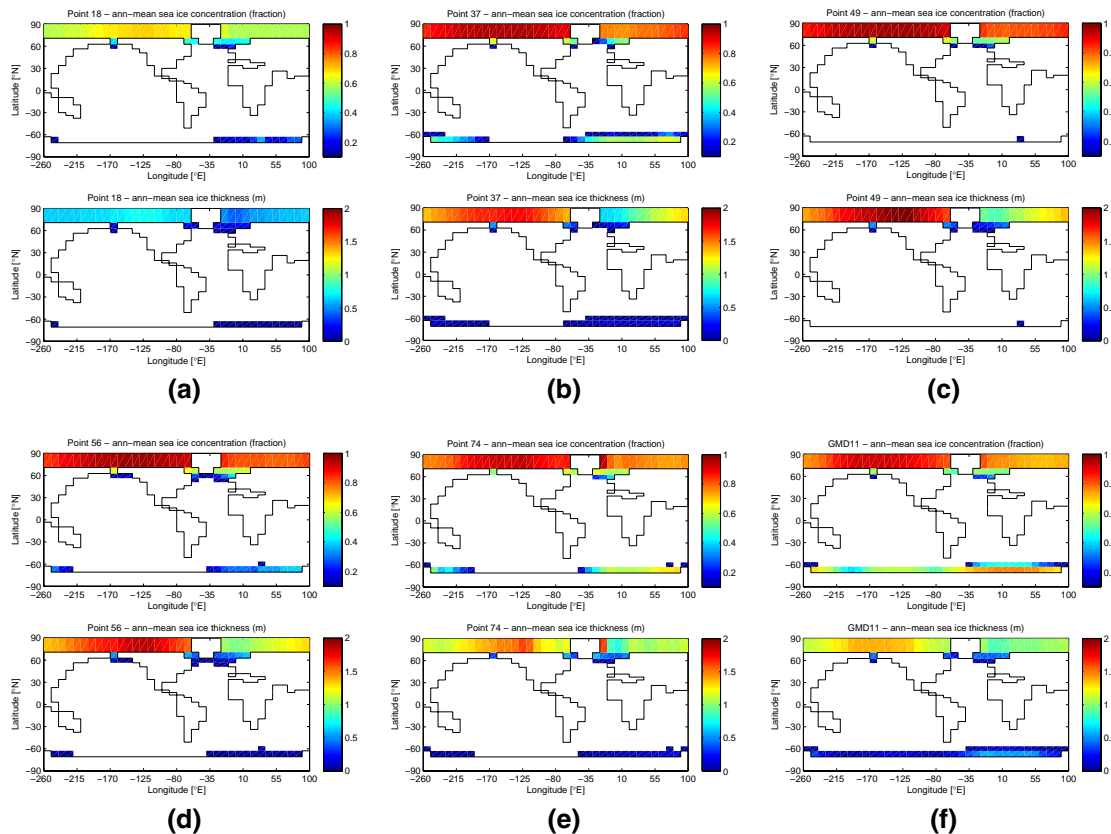



Fig. 4. Sea ice – (a) point no. 18, (b) point no. 37, (c) point no. 49, (d) point no. 56, (e) point no. 74, and (f) GMD11.

[Title Page](#)

[Abstract](#) [Introduction](#)

[Conclusions](#) [References](#)

[Tables](#) [Figures](#)

[◀](#) [▶](#)

[◀](#) [▶](#)

[Back](#) [Close](#)

[Full Screen / Esc](#)

[Printer-friendly Version](#)

[Interactive Discussion](#)



An optimally tuned
GENIE ensemble

R. Marsh et al.

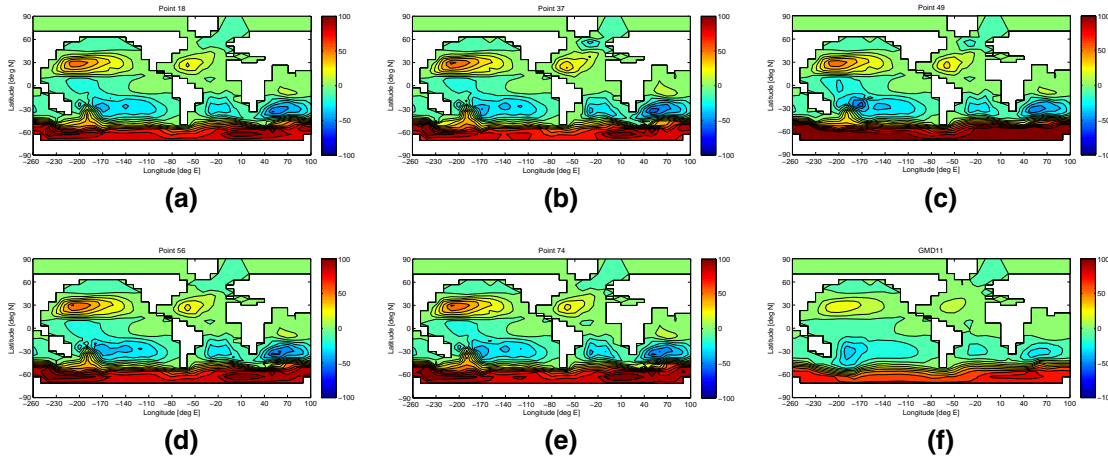


Fig. 5. Barotropic stream function – (a) point no. 18, (b) point no. 37, (c) point no. 49, (d) point no. 56, (e) point no. 74, and (f) GMD11.

Title Page

Abstract

Introduction

Conclusions

References

Tables

Figures

◀

▶

◀

▶

Back

Close

Full Screen / Esc

Printer-friendly Version

Interactive Discussion



An optimally tuned
GENIE ensemble

R. Marsh et al.

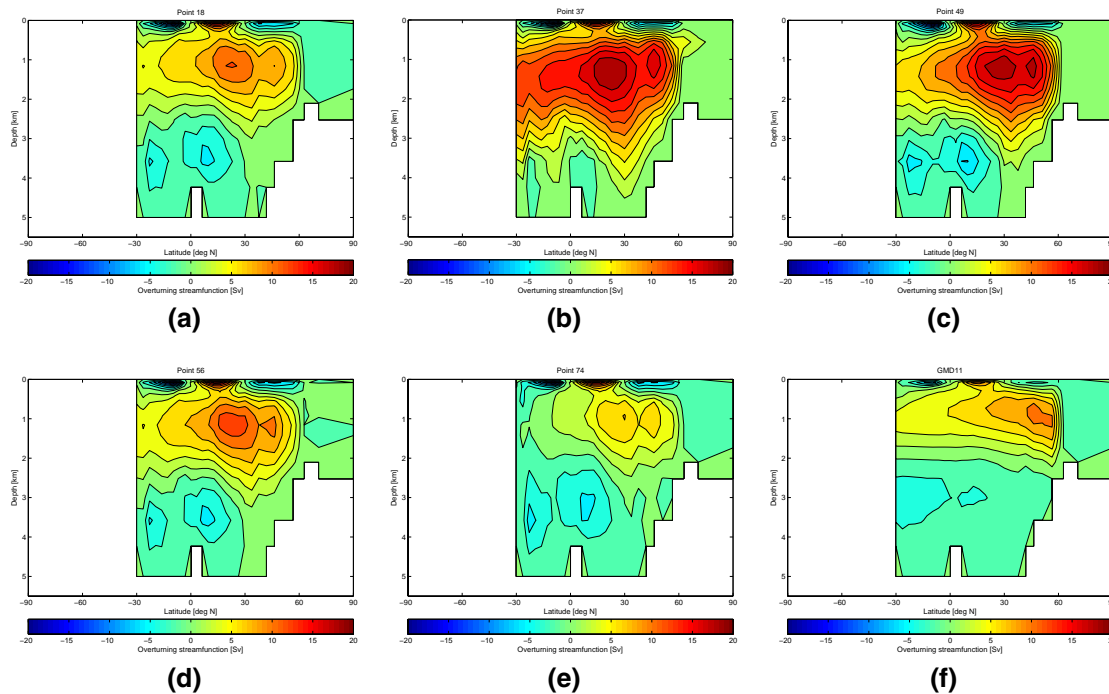


Fig. 6. Atlantic overturning streamfunction – (a) point no. 18, (b) point no. 37, (c) point no. 49, (d) point no. 56, (e) point no. 74, and (f) GMD11.

Title Page

Abstract

Introduction

Conclusions

References

Tables

Figures

◀

▶

◀

▶

Back

Close

Full Screen / Esc

Printer-friendly Version

Interactive Discussion



An optimally tuned GENIE ensemble

R. Marsh et al.

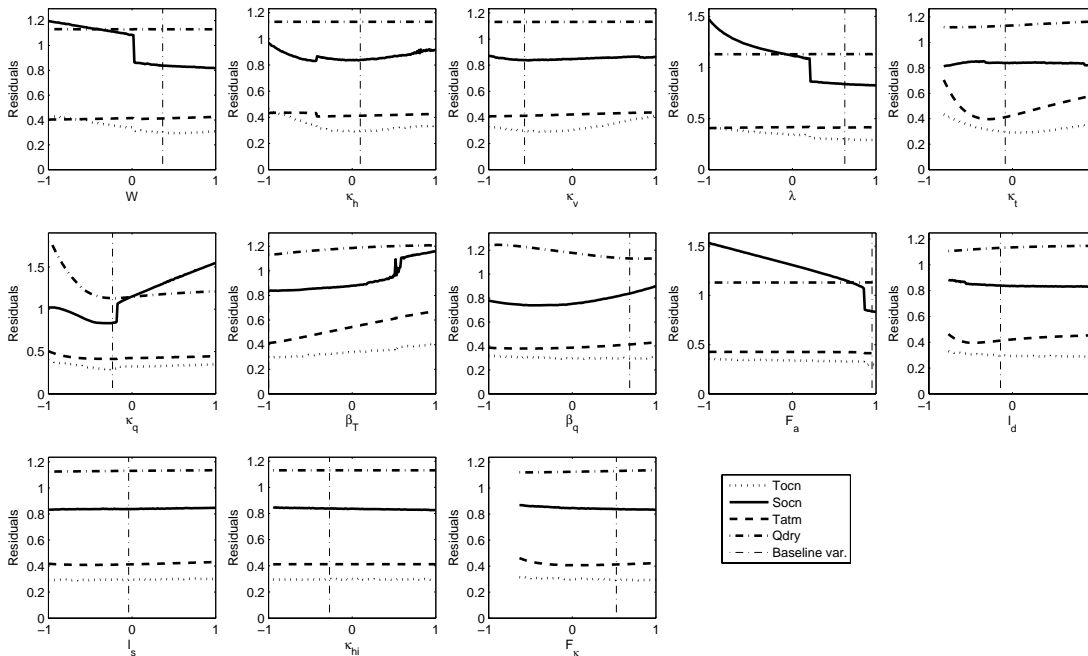


Fig. 7. 1-D slices through the objective function landscapes around point 18. The parameter axes are non-dimensionalised, -1 and 1 representing the minima and maxima of the input parameter values (Table 1), respectively.

Title Page

Abstract

Introduction

Conclusions

References

Tables

Figures

◀

▶

◀

▶

Back

Close

Full Screen / Esc

Printer-friendly Version

Interactive Discussion



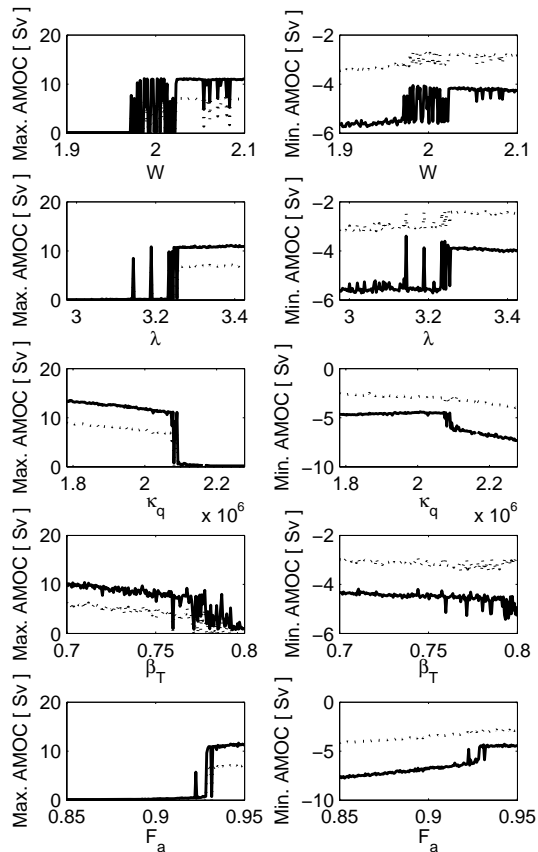


Fig. 8. 1-D slices showing the maximum (left panels) and minimum (right panels), overturning streamfunction in the Atlantic, excluding near-surface wind-driven cells (left panel), in the vicinity point 18. The minimum AMOC is equivalent to the maximum in the Antarctic cell in the Atlantic. The dotted lines refer to the AMOC maxima and minima at the Equator in the Atlantic.

An optimally tuned
GENIE ensemble

R. Marsh et al.

Title Page

Abstract

Introduction

Conclusions

References

Tables

Figures

◀

▶

◀

▶

Back

Close

Full Screen / Esc

Printer-friendly Version

Interactive Discussion

